Sensorless Control of Permanent Magnet Synchronous Machine Based on Second-Order Sliding-Mode Observer With Online Resistance Estimation

Donglai Liang, *Student Member, IEEE*, Jian Li, *Member, IEEE*, and Ronghai Qu, *Senior Member, IEEE*

***Abstract*—In this paper, a supertwisting algorithm based second-order sliding-mode observer (STA-SMO) with online stator resistance (R_s) estimation for sensorless control of a nonsalient permanent magnet synchronous machine is proposed. A stator current observer is designed based on an STA to estimate the back electromotive force. A discontinuous sign function in the conventional SMO is replaced by a supertwisting function. The chattering problem, unavoidable in conventional SMO, is eliminated by reducing the amplitude of switching function of an STA-SMO. Meanwhile, a parallel online R_s estimation scheme is presented based on a modified SMO. Because mismatch between actual and set resistance may lead to estimation error and even system instability. The Lyapunov stability theorem is used to obtain the stable conditions of the proposed online R_s observer at both motoring and generating mode. With the help of online R_s observer, resistance uncertainties caused by temperature variation can be taken into account, which means robustness and stability of an STA-SMO can be improved. At the same time, higher position and speed estimation accuracy is obtained and operation range of sensorless control is extended. Finally, the proposed method is validated and compared with a conventional method by simulations and experiments.**

***Index Terms*—Online resistance estimation, permanent magnet synchronous machine (PMSM), second order, sensorless control, sliding-mode observer (SMO), supertwisting algorithm (STA).**

I. Introduction

RECENTLY, the application of permanent magnet synchronous machine (PMSM) is increasing rapidly in industrial area. One of the most popular control methods is field-oriented control, which requires accurate rotor position. Generally, accurate rotor position can be obtained by an encoder or resolver. However, these devices are expensive and unreliable in some rugged environment. Besides, in some compact design, there is no extra installation space. Therefore, sensorless control is gaining more and more attention. Sensorless techniques are divided into two categories, one is based on machine anisotropy [1]–[3], and the other is based on the mathematical model of PMSM [4]–[15].

Anisotropy-based techniques are suitable for low speed and zero speed sensorless operation. Rotor position is acquired by injecting high-frequency (HF) signals into the machine. However, injected HF signals can produce more losses and larger torque ripple. Mathematical model based methods are suitable for medium and high speed sensorless operation. Rotor position and speed are obtained by estimating back electromotive force (back EMF). It has been considered to be a standard sensorless solution in industrial area [16]. Whole speed range sensorless operation can be achieved by combining machine anisotropy based methods with machine model based methods [17]. However, a hybrid sensorless control system will increase complexity of the system.

Many researchers have made contributions to model-based sensorless control methods, such as model reference adaptive system (MRAS) [4], extended Kalman filter (EKF) [5], [6], sliding-mode observer (SMO) [7]–[15], etc. In [4], an MRAS-based sensorless control with online parameter estimation for interior PMSM is proposed. Position and speed estimation accuracy is improved greatly with the aid of an estimation scheme. In [5], a hysteresis hybrid observer that combines an EKF with hybrid automation is proposed for wide speed sensorless operation. The hysteresis is introduced to avoid chattering at ultralow speed. In [6], a position observer comprising augmented EKF and another EKF is proposed for electromagnetic valve actuator sensorless control. At the same time, a machine parameter is estimated to obtain higher position estimation accuracy. In [9] and [18], a two-stage high-gain observer is proposed to overcome parameters uncertainties and avoid difficult estimation in PMSM sensorless control.

An SMO is widely used for sensorless control due to its easy implementation and robustness against parameters variation. A conventional SMO suffers from chattering problem that is caused by the sign function. A low-pass filter (LPF) is widely

Manuscript received November 30, 2016; revised March 7, 2017; accepted March 27, 2017. Date of publication March 31, 2017; date of current version July 15, 2017. Paper 2016-IDC-1323.R1, presented at the 2016 IEEE Energy Conversion Congress and Exposition, Milwaukee, WI, USA, September 18–22, and approved for publication in the IEEE TRANSACTIONS ON INDUSTRY APPLICATIONS, by the Industrial Drives Committee of the IEEE Industry Applications Society. *(Corresponding author: Jian Li.)*

The authors are with the State Key Laboratory of Advanced Electromagnetic Engineering and Technology, School of Electrical and Electronic Engineering, Huazhong University of Science and Technology, Wuhan 430074, China (e-mail: liangdonglai@hust.edu.cn; jianli@hust.edu.cn; ronghaiqu@mail.hust.edu.cn).

Color versions of one or more of the figures in this paper are available online at http://ieeexplore.ieee.org.

Digital Object Identifier 10.1109/TIA.2017.2690218

employed in the first-order SMO to reduce the chattering problem. However, an LPF brings the problem of gain attenuation and phase delay [7]. In order to reduce the chattering problem, sigmoid function is proposed to replace the sign function in [8]. Nonetheless, phase compensation is still necessary due to the existence of LPF. Higher order SMO is one of the solutions which can eliminate chattering and does not compromise robustness [19]. A supertwisting algorithm based second-order SMO (STA-SMO) is proposed to eliminate the chattering by using auxiliary surfaces [20], [21]. Then, a strong Lyapunov function is obtained for the STA, which simplifies the analysis of the second-order SMO and gives the stable conditions of the STA-SMO [22]. The STA-SMO with online stator winding resistance (R_s) estimation for sensorless control of an induction machine is proposed in [19] to improve robustness and performance of low speed range operation. Basic research on the STA-SMO for PMSM sensorless control are introduced in [23] and [24]. However, only simulation results are presented and the impact of parameters variation is ignored, which may lead to system instability.

Online R_s estimation plays an important role in sensorless control, especially in low speed region, where back EMF is relatively small compared to voltage drop across R_s [25]. Mismatch between actual and set value of R_s may lead to rotor position and speed estimation error. Especially, this mismatch may result in system instability of the STA-SMO if large estimation error occurs. Several measures can be used to estimate R_s online. A first-order SMO with online R_s estimation is proposed for PMSM sensorless control [8]. Back EMF and R_s are estimated at the same time. In [19], an MRAS-based R_s estimation scheme is proposed to improve the sensorless control performance of an induction machine. The sensorless operation range is extended by online estimating R_s. An online R_s estimation method is proposed in [26], by injecting $i_d \neq 0$ into the *d*-axis current, R_s is estimated with high accuracy, but the effect of injected current on drive system is ignored. In [27], R_s is estimated at steady state based on the addition of rotor position offsets and neural network, but estimating R_s at dynamic state is invalid.

In this paper, an STA-SMO with online R_s estimation is proposed for surface-mounted PMSM sensorless control. Traditional sign function is replaced by supertwisting function to eliminate chattering. It was found out that stator resistance variation may lead not only to position estimation error, but also to system instability if large estimation error occurs. Then, an online R_s estimation scheme is proposed based on a modified first-order SMO to overcome the resistance uncertainties. Stable conditions of the R_s observer is obtained with the help of the Lyapunov stability theorem. R_s is estimated without injecting any signal and modified SMO is easier to be implemented on microprocessor than neural network. By combining the STA-SMO with online R_s estimation, estimation accuracy, system stability, and robustness of the system have been improved. Besides, sensorless operation has been extended to lower speed region. Finally, both simulations and experiments are conducted to validate the effectiveness of the proposed sensorless technique.

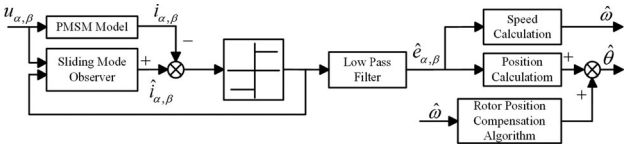

Fig. 1. Conventional sliding-mode observer for PMSM sensorless control.

II. Conventional Sliding-Mode Observer

Assuming that the surface-mounted PMSM has symmetrical structure, symmetrical three-phase current, and the iron losses, eddy-current losses and saturation effect are ignored. The $\alpha\beta$-axis voltage equations can be expressed as follows:

$$\frac{di_\alpha}{dt} = -\frac{R_s}{L_s} i_\alpha + \frac{1}{L_s} u_\alpha - \frac{1}{L_s} e_\alpha \tag{1a}$$

$$\frac{di_\beta}{dt} = -\frac{R_s}{L_s} i_\beta + \frac{1}{L_s} u_\beta - \frac{1}{L_s} e_\beta \tag{1b}$$

where $i_{\alpha\beta}$, $u_{\alpha\beta}$, and $e_{\alpha\beta}$ represent the current, voltage, and back EMF in stationary reference frame, respectively. R_s and L_s represent the stator winding resistance and inductance, respectively. The PMSM is working at linear region and stator inductance variation is neglected. Therefore, the inductance in the $\alpha\beta$-axis are assumed to be constant throughout this paper.

The basic idea of the conventional SMO is introduced in [28]. The Lyapunov stability theorem can be used to obtain the stable conditions of conventional SMO. An equivalent control method is used to calculate the estimated back EMF for sensorless operation [29]. The estimation algorithm is shown in Fig. 1. The chattering problem is mainly caused by sign function, which is used to estimate back EMF. Although, an LPF can reduce the chattering, it also brings phase delay and gain attenuation.

III. Second-Order Sliding-Mode Observer Based on Supertwisting Algorithm

A. Supertwisting Algorithm

A supertwisting algorithm is proposed by Levant in [20] and [30]. The purpose of the STA is to eliminate the chattering problem in the first-order SMO. A strong Lyapunov function is obtained to prove the stability and finite time convergence of the STA in [22] and [31]. The basic form of the STA with perturbation is designed as

$$\begin{aligned} \frac{dx_1}{dt} &= -k_1 |\bar{x}_1|^{1/2} \text{sign}(\bar{x}_1) + x_2 + \rho_1(x_1, t) \\ \frac{dx_2}{dt} &= -k_2 \text{sign}(\bar{x}_1) + \rho_2(x_2, t) \end{aligned} \tag{2}$$

where $x_i, \bar{x}_i (\bar{x}_i = \hat{x}_i - x_i), k_i, \rho_i$, and sign() are state variables, error between estimated and actual values, sliding coefficients, perturbation terms, and sign function, respectively.

It has been proved in [22] that if the perturbation terms in (2) are globally bounded by

$$|\rho_1| \leqslant \delta_1 |x_1|^{1/2}, \ \rho_2 = 0 \tag{3}$$

and the gains k_1 and k_2 satisfy

$$k_1 > 2\delta_1,\ k_2 > k_1 \frac{5\delta_1 k_1 + 4\delta_1^2}{2(k_1 - 2\delta_1)} \tag{4}$$

then the system will converge in finite time to sliding surface, where δ_1 is any positive constant.

B. STA-SMO for PMSM Sensorless Control

In order to obtain the estimated rotor position, a stator current observer is designed based on the STA-SMO. Take the estimated $\alpha\beta$-axis currents $\hat{i}_\alpha$ and $\hat{i}_\beta$ as state variables and substituting $x_1 = \hat{i}_\alpha$ and $x_1 = \hat{i}_\beta$ into (2), respectively. Equation (2) can be rewritten as

$$\frac{d\hat{i}_\alpha}{dt} = -k_1 |\bar{i}_\alpha|^{1/2} \text{sign}(\bar{i}_\alpha) - \int k_2 \text{sign}(\bar{i}_\alpha) dt + \rho_1(\hat{i}_\alpha, t) \tag{5a}$$

$$\frac{d\hat{i}_\beta}{dt} = -k_1 |\bar{i}_\beta|^{1/2} \text{sign}(\bar{i}_\beta) - \int k_2 \text{sign}(\bar{i}_\beta) dt + \rho_1(\hat{i}_\beta, t). \tag{5b}$$

The perturbation terms $\rho_1(\hat{i}_\alpha, t)$ and $\rho_1(\hat{i}_\beta, t)$ are designed as

$$\begin{aligned} \rho_1(\hat{i}_\alpha, t) &= -\frac{R_s}{L_s}\hat{i}_\alpha + \frac{1}{L_s}u_\alpha \\ \rho_1(\hat{i}_\beta, t) &= -\frac{R_s}{L_s}\hat{i}_\beta + \frac{1}{L_s}u_\beta \end{aligned} \tag{6}$$

then the current observer can be expressed as

$$\begin{aligned} \frac{d\hat{i}_\alpha}{dt} &= -\frac{R_s}{L_s}\hat{i}_\alpha + \frac{1}{L_s}u_\alpha + \frac{1}{L_s}k_1 |\bar{i}_\alpha|^{1/2} \text{sign}(\bar{i}_\alpha) \\ &\quad + \frac{1}{L_s}\int k_2 \text{sign}(\bar{i}_\alpha) dt \end{aligned} \tag{7a}$$

$$\begin{aligned} \frac{d\hat{i}_\beta}{dt} &= -\frac{R_s}{L_s}\hat{i}_\beta + \frac{1}{L_s}u_\beta + \frac{1}{L_s}k_1 |\bar{i}_\beta|^{1/2} \text{sign}(\bar{i}_\beta) \\ &\quad + \frac{1}{L_s}\int k_2 \text{sign}(\bar{i}_\beta) dt. \end{aligned} \tag{7b}$$

It should be noticed that the perturbation terms ρ_1 in (2) is replaced by $-\frac{R_s}{L_s}i_\alpha + \frac{1}{L_s}u_\alpha$ and $-\frac{R_s}{L_s}i_\beta + \frac{1}{L_s}u_\beta$, respectively.

Substituting (6) into (3) and replacing x_1 by the estimated $\alpha\beta$-axis currents $\hat{i}_\alpha$ and $\hat{i}_\beta$, respectively. Equation (3) can be rewritten as

$$\begin{aligned} -\frac{R_s}{L_s}\hat{i}_\alpha + \frac{1}{L_s}u_\alpha - \delta_1 |\hat{i}_\alpha|^{1/2} \leqslant 0 \\ -\frac{R_s}{L_s}\hat{i}_\beta + \frac{1}{L_s}u_\beta - \delta_1 |\hat{i}_\beta|^{1/2} \leqslant 0. \end{aligned} \tag{8}$$

For a large enough δ_1, the above inequality can be satisfied easily.

By subtracting (1) from (7), the state equations of the $\alpha\beta$-axis currents errors are derived:

$$\begin{aligned} \frac{d\bar{i}_\alpha}{dt} &= -\frac{R_s}{L_s}\bar{i}_\alpha + \frac{1}{L_s}(k_1 |\bar{i}_\alpha|^{1/2} \text{sign}(\bar{i}_\alpha) \\ &\quad + \int k_2 \text{sign}(\bar{i}_\alpha) dt + e_\alpha) \\ \frac{d\bar{i}_\beta}{dt} &= -\frac{R_s}{L_s}\bar{i}_\beta + \frac{1}{L_s}(k_1 |\bar{i}_\beta|^{1/2} \text{sign}(\bar{i}_\beta) \\ &\quad + \int k_2 \text{sign}(\bar{i}_\beta) dt + e_\beta). \end{aligned} \tag{9}$$

When the system is stable, the estimation errors are on the sliding surface, which means the estimated value is close to the actual value ($\hat{i}_\alpha \approx 0$, $\hat{i}_\beta \approx 0$). Then, the equivalent control method can be used to obtain the estimated back EMF e_α and e_β as follows [29]:

$$\begin{aligned} e_\alpha &= -k_1 |\bar{i}_\alpha|^{1/2} \text{sign}(\bar{i}_\alpha) - \int k_2 \text{sign}(\bar{i}_\alpha) dt) \\ e_\beta &= -k_1 |\bar{i}_\beta|^{1/2} \text{sign}(\bar{i}_\beta) - \int k_2 \text{sign}(\bar{i}_\beta) dt). \end{aligned} \tag{10}$$

C. Stability Discussion

Stable operation of the system requires small estimated rotor position and speed errors. However, in practice, stator parameters may change. For example, R_s may change due to temperature variation, which will bring position estimation error. Furthermore, large estimation error may result in unstable operation of the system, especially at low speed range, where back EMF is low. For example, assuming that the ambient temperature is 20 °C and temperature rise in machine is 70 °C. The resistivity of copper increases from 1.7×10^{-8} to 2.3×10^{-8} Ω·m. It means that the stator resistance and voltage drop across stator resistance increase by 35%. This variation is too large that it may result in system instability due to large estimation error. Therefore, an online R_s estimation is necessary. An online R_s estimation helps us to obtain an accurate machine model, which can improve the estimation accuracy and stability of the STA-SMO. Impact of resistance variation on system stability can be ignored by estimating R_s. Details of an online R_s estimation scheme will be introduced in Section IV.

At steady state, the impact of inductance variation on system stability can be ignored, because $L_s di_{\alpha\beta}/dt$ is much smaller than $R_s i_{\alpha\beta}$. Therefore, the influence of inductance variation on system stability is not discussed here.

D. Position and Speed Calculation

Since $\hat{e}_\alpha$ and $\hat{e}_\beta$ can be expressed as

$$\begin{aligned} \hat{e}_\alpha &= -\psi_f \hat{\omega} \sin\hat{\theta} \\ \hat{e}_\beta &= \psi_f \hat{\omega} \cos\hat{\theta}. \end{aligned} \tag{11}$$

Then, the estimated rotor position and speed can be calculated by

$$\hat{\theta} = \arccos\left(\hat{e}_\alpha / \sqrt{\hat{e}_\alpha^2 + \hat{e}_\beta^2}\right)$$
$$\hat{\omega} = \text{LPF}(d\hat{\theta}/dt). \tag{12}$$

Rotor position can be also obtained by $\arctan(-\hat{e}_\alpha/\hat{e}_\beta)$, but estimation noise may bring estimation error when $\hat{e}_\beta$ is close to zero. Employment of trigonometric function $\arccos()$ in (12) can alleviate the influence of estimation noise. A first-order LPF is used to obtain a smooth rotor speed signal. The LPF for rotor speed calculation is designed as $\omega_c/(s+\omega_c)$. The cutoff frequency of the LPF should be selected based on the maximum rotor speed and switching frequency.

E. Discrete STA-SMO

The sensorless control scheme must be discretized to be implemented on microprocessor. A discrete-time STA-SMO can be written as (the Euler scheme)

$$\hat{i}_x(k) = T\frac{u_x(k-1)}{L_s} + \left(1 - \frac{\hat{R}_s}{L_s}T\right)\hat{i}_x(k-1) + T\frac{\hat{e}_x(k-1)}{L_s}$$
$$\hat{e}_x(k) = k_1|\bar{i}_x(k-1)|^{1/2}\cdot\text{sign}(\bar{i}_x(k-1)) + z_x(k-1)$$
$$z_x(k) = z_x(k-1) + Tk_2\cdot\text{sign}(\bar{i}_x(k))$$

where x denotes the $\alpha\beta$-axis, T is the sampling period, $\hat{R}_s$ is the estimated stator resistance, k is the index of discrete sampling instant, and $\bar{i}_x(k) = \hat{i}_x(k) - i_x(k)$.

After discretization, the performance of the STA-SMO will deteriorate due to limited sampling time. More chattering will appear in the estimation results. However, chattering of the STA-SMO is still much smaller than that of the first-order SMO if the same Euler scheme is used for discretization. This has been verified by experiments in Section VI. Besides, stable conditions of a continuous system are necessary but not sufficient after discretization [32]. The necessary and sufficient conditions for stable operation of a discrete STA-SMO are presented as follows:

$$[\bar{i}_x(k+1) - \bar{i}_x(k)]\text{sign}(\bar{i}_x(k)) < 0$$
$$[\bar{i}_x(k+1) + \bar{i}_x(k)]\text{sign}(\bar{i}_x(k)) \geqslant 0.$$

In [32], stable conditions for a discrete STA-SMO are obtained with the help of the Lyapunov stability theorem. In this paper, if the sliding-mode coefficients k_1 and k_2 are selected based on the conditions presented in [32] and under the constraint of the above necessary and sufficient conditions, the discrete STA-SMO will be stable.

The STA-SMO for PMSM sensorless control is shown in Fig. 2. Compared to a first-order SMO presented in Fig. 1, the first-order LPF and rotor position compensation algorithm are eliminated, which can reduce the complexity of sensorless control system.

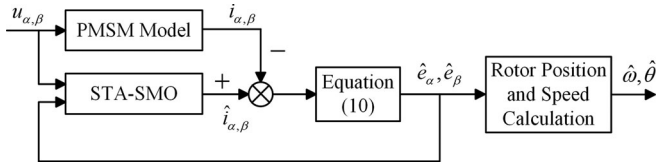

Fig. 2. Block diagram of an STA-SMO.

IV. Online Stator Winding Resistance Estimation

A. Online R_s Estimation Scheme Based on Modified SMO

The dq-axis voltage equations of PMSM can be expressed as follows:

$$\frac{di_d}{dt} = \frac{u_d}{L_s} + \hat{\omega}i_q - \frac{R_s}{L_s}i_d \tag{13a}$$
$$\frac{di_q}{dt} = \frac{u_q}{L_s} - \hat{\omega}i_d - \frac{\hat{\omega}}{L_s}\psi_f - \frac{R_s}{L_s}i_q \tag{13b}$$

where i_{dq} and u_{dq} are stator current and voltage in rotating reference frame, respectively, $\hat{\omega}$ is the estimated rotor speed obtained by the STA-SMO. Both d-axis and q-axis voltage equations contain R_s. Assuming that both equations can be used to estimate R_s. The modified stator current observers are constructed as follows:

$$\frac{d\hat{i}_d}{dt} = \frac{u_d}{L_s} + \hat{\omega}i_q - \frac{k_R\cdot\text{sign}(\hat{i}_d - i_d)}{L_s}i_d \tag{14a}$$
$$\frac{d\hat{i}_q}{dt} = \frac{u_q}{L_s} - \hat{\omega}i_d - \frac{\hat{\omega}}{L_s}\psi_f - \frac{k_R\cdot\text{sign}(\hat{i}_q - i_q)}{L_s}i_q \tag{14b}$$

where k_R is the sliding-mode coefficient of the proposed R_s observer. Different from the conventional first-order SMO mentioned in [8, eq. (3)], the state variables i_d and i_q in the last term of (14) are actual currents, instead of estimated currents. Otherwise, stable condition cannot be obtained using the Lyapunov stability theorem, and R_s cannot be estimated by the conventional SMO.

In rotating reference frame, (13a) and (13b) are decoupled, which means that only one equation is sufficient to estimate R_s . Since $i_d = 0$ a field-oriented control method is employed in this paper, it is difficult to estimate R_s in the d-axis voltage equation when $i_d = 0$. Thus, (13b) and (14b) are considered only.

The state equation of the estimation errors $\bar{i}_q(\bar{i}_q = \hat{i}_q - i_q)$ can be derived by subtracting (13b) from (14b):

$$\frac{d\bar{i}_q}{dt} = \frac{R_s}{L_s}i_q - \frac{k_R\cdot\text{sign}(\bar{i}_q)}{L_s}i_q. \tag{15}$$

When the sliding mode is reached, the estimated error is on the sliding surface, which means the estimated value is close to the actual value ($\bar{i}_q \approx 0$). The estimated R_s can be obtained by an equivalent control method. It can be seen that R_s is equivalent to $k_R\cdot\text{sign}(\bar{i}_q)$. The estimated stator winding resistance $\hat{R}_s$ can be derived by a first-order LPF as follows:

$$\hat{R}_s = \text{LPF}(k_R\cdot\text{sign}(\bar{i}_q)). \tag{16}$$

The LPF is the same as that shown in Section III-D.

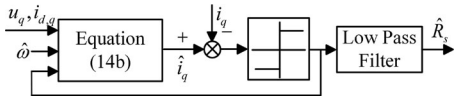

Fig. 3. Block diagram of the online R_s estimation scheme.

B. Stability Analysis

The sliding surface is defined as function of the error between estimated and actual value as follows:

$$S = \hat{i}_q - i_q \tag{17}$$

For R_s estimation, the Lyapunov function used to find the sliding condition is defined as

$$V = \frac{1}{2} S^T S. \tag{18}$$

The sliding condition can be derived from the Lyapunov stability theorem [33]. The observer is stable only if $\dot{V} < 0$ for $V > 0$. The time differential equation of (18) is given as

$$\frac{dV}{dt} = S \cdot \frac{dS}{dt} = \bar{i}_q \cdot \frac{d\bar{i}_q}{dt}. \tag{19}$$

By substituting (15) into (19), the sliding condition can be expressed as

$$\frac{dV}{dt} = (\hat{i}_q - i_q) i_q \left(\frac{R_s - k_R \cdot \text{sign}(\hat{i}_q - i_q)}{L_s} \right) < 0. \tag{20}$$

Since the field-oriented control is based on $i_d = 0$, i_q must be positive to produce positive torque.

When $\hat{i}_q \geqslant i_q$, (20) can be rewritten as

$$\frac{dV}{dt} = (\hat{i}_q - i_q) i_q \left(\frac{R_s - k_R}{L_s} \right) < 0. \tag{21}$$

Therefore, the sliding-mode condition to satisfy $\dot{V} < 0$ is $k_R > R_s$ and $i_q > 0$.

When $\hat{i}_q < i_q$, (20) can be rewritten as

$$\frac{dV}{dt} = (\hat{i}_q - i_q) i_q \left(\frac{R_s + k_R}{L_s} \right) < 0. \tag{22}$$

Therefore, the sliding-mode condition to satisfy $\dot{V} < 0$ is $k_R > -R_s$ and $i_q > 0$.

Thus, the sliding-mode condition for motoring mode is summarized as follows:

$$k_R > R_s \text{ and } i_q > 0.$$

For generating mode, stable conditions can be obtained using the same way, the stable conditions is given as follows:

$$k_R < -R_s \text{ and } i_q < 0.$$

The diagram of the online R_s estimation is shown in Fig. 3. It can be seen that the estimation process is similar to the conventional SMO for PMSM sensorless drives shown in Fig. 1. A first-order LPF is also employed in R_s estimation scheme. Since R_s is mainly influenced by temperature, which varies much slower than stator winding currents. Therefore, phase delay caused by an LPF is negligible and a simple first-order SMO is sufficient for estimating R_s. The STA-SMO with online R_s estimation for PMSM sensorless control is shown in Fig. 4. R_s is estimated in rotating reference frame. The dq-axis currents and reference voltages are used for R_s estimation.

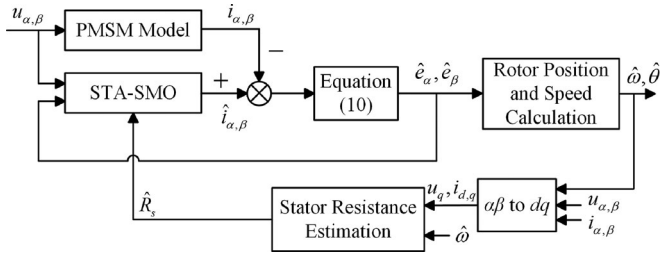

Fig. 4. STA-SMO with the online R_s estimation scheme.

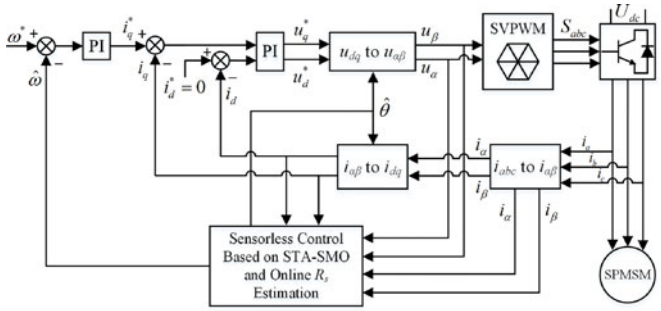

Fig. 5. Block diagram of sensorless field-oriented control for PMSM.

TABLE I
MAIN PARAMETERS OF PMSM AND CONTROL SYSTEM

Items	Value	Items	Value
Stator resistance (Ω)	0.735	Rated phase current (A)	10.6
Rotor flux linkage (Wb)	0.1385	DC bus voltage (V)	150
Stator inductance (mH)	10.24	Rated speed (r/min)	300
Pole pairs	10	k_1	2
Rated power (kW)	7	k_2	3000
Rated torque (N·m)	20	k_R	2

V. Simulation Results and Discussions

The system diagram of sensorless control with an online R_s estimation scheme is shown in Fig. 5. $i_d = 0$ field-oriented control method is applied in this paper. Space-vector pulse width modulation is employed to enhance the utilization of dc bus voltage. The details of the sensorless control and online R_s estimation scheme is shown in Figs. 3 and 4, respectively. Table I gives the main parameters of PMSM and control system.

A. Simulation Results of the Conventional SMO and STA-SMO

Both of the conventional first-order SMO and STA-SMO based sensorless control systems are constructed under continuous-time domain and the system bandwidth is the same.

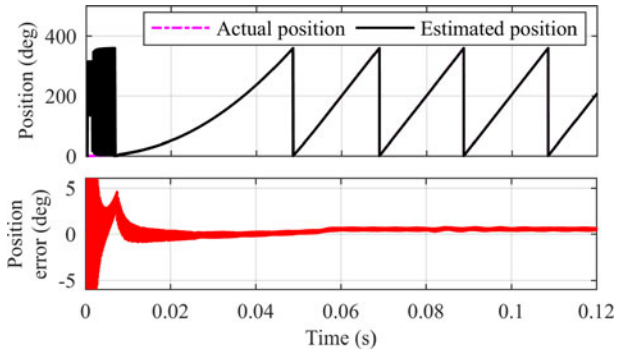

Fig. 6. Rotor position and position error of the conventional first-order SMO for PMSM sensorless control (accelerate from 0 speed to 300 r/min).

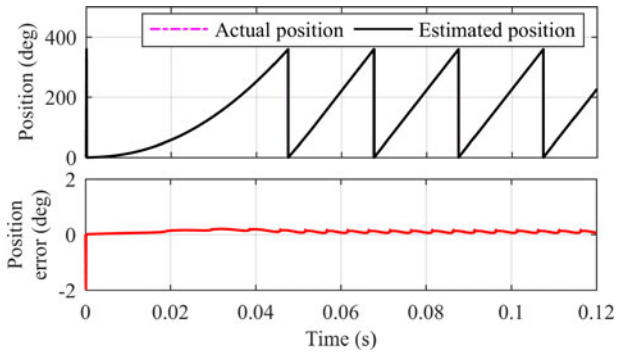

Fig. 7. Rotor position and position error of an STA-SMO for PMSM sensorless control (accelerate from 0 speed to 300 r/min).

The machine is accelerated from 0 speed to 300 r/min by sensorless control with a 10 N·m load. Simulation results of the conventional first-order SMO and STA-SMO are shown in Figs. 6 and 7, respectively. Comparing the relative position error, the chattering problem is eliminated, especially for low speed operation range. For the conventional first-order SMO, chattering is caused by switching function. Large chattering at low speed may cause not only large estimation error, but also system instability. However, the amplitude of the switching function is reduced in the STA-SMO, which can reduce chattering greatly. Therefore, an STA-SMO is presented in this paper to improve the performance of PMSM sensorless control.

B. Simulation Results of STA-SMO Without Online R_s Estimation

The simulation results of STA-SMO sensorless control without online R_s estimation is shown in Fig. 8. There is a step change in R_s from 0.735 to 1.068 Ω at 0.4 s. Meanwhile, the PMSM is accelerated from 0 speed to 60 r/min with a 10 N·m load.

It is obvious that there is a large steady-state error between actual and estimated rotor speed when step change in R_s happens. After the step change, the actual rotor speed cannot converge to reference value due to the wrong estimated rotor speed. Besides, position chattering occurs after R_s is changed, which also produces serious torque ripple. In the real world, these problem

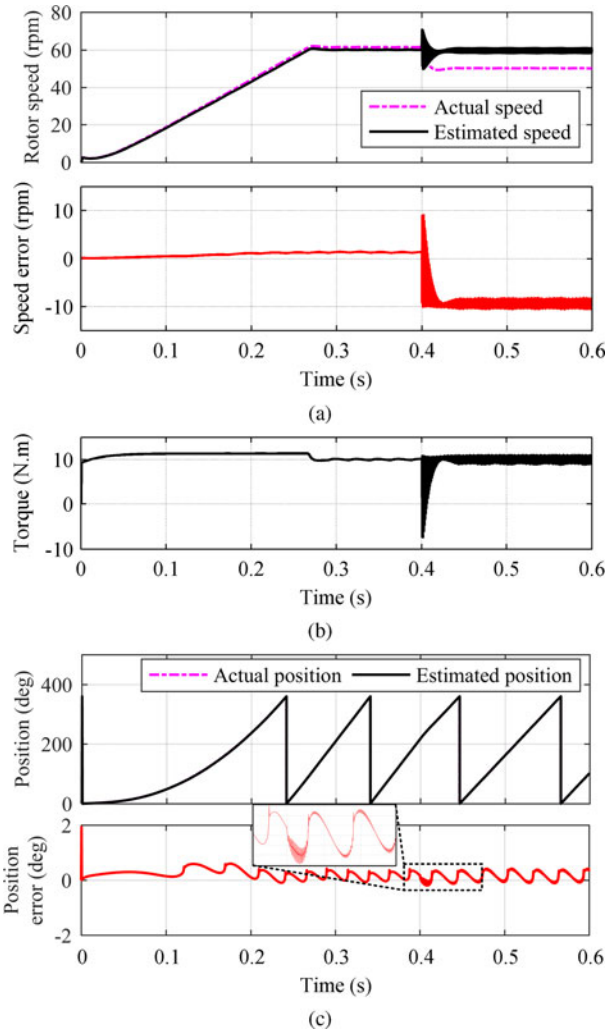

Fig. 8. STA-SMO without online R_s estimation for PMSM sensorless control. (a) Rotor speed and speed error, (b) torque, and (c) rotor position and position error.

will be exaggerated by discretization and measurement noises. Larger estimation error and even instability may occur. Therefore, online estimating R_s is necessary in terms of estimation accuracy and system stability.

C. Simulation Results of STA-SMO With Online R_s Estimation

The simulation results of the STA-SMO after applying the proposed online R_s estimation scheme is shown in Fig. 9. The system configuration is the same as that without R_s estimation. In Fig. 9(d), the online R_s observer tracks the actual R_s successfully. After R_s is changed, the chattering problem in estimated position is eliminated. Besides, rotor speed error is reduced to zero and ripple in electromagnetic torque is eliminated. Since the PMSM is accelerated from standstill, the stator winding observer needs a very short time to converge to actual value. Therefore, the position and speed error will be a little bit larger at the beginning. Estimation error at the beginning can be ignored when the estimated stator winding resistance converges to the actual value of R_s.

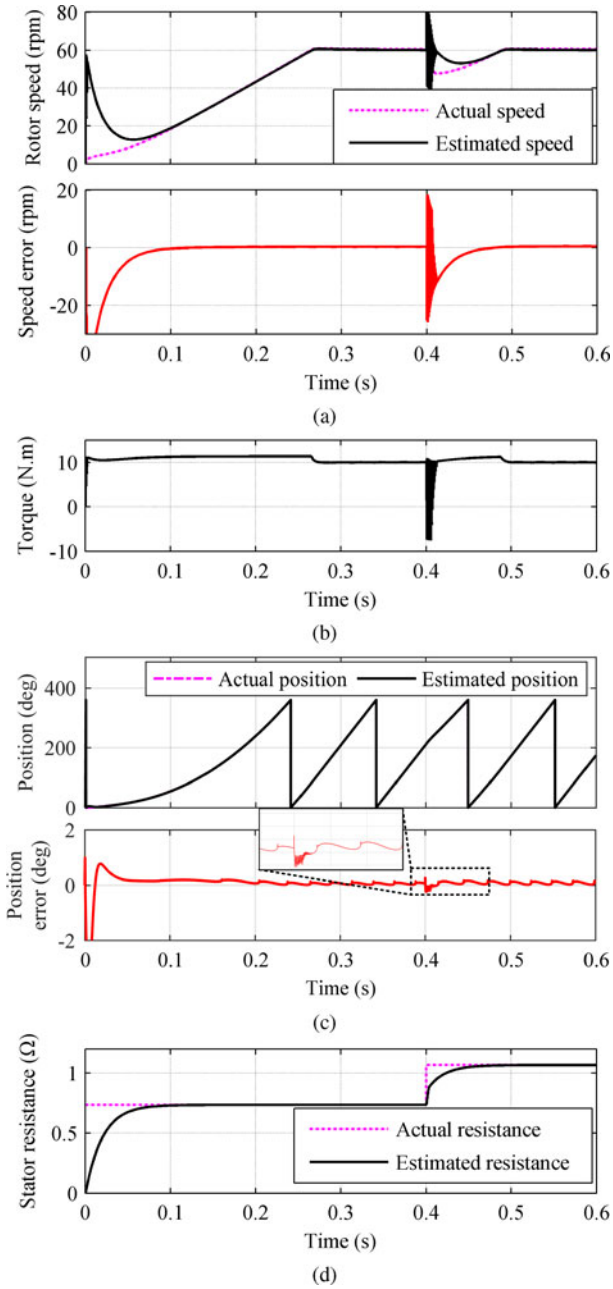

Fig. 9. STA-SMO with online R_s estimation for PMSM sensorless control. (a) Rotor speed and speed error, (b) torque, (c) rotor position and position error, and (d) resistance.

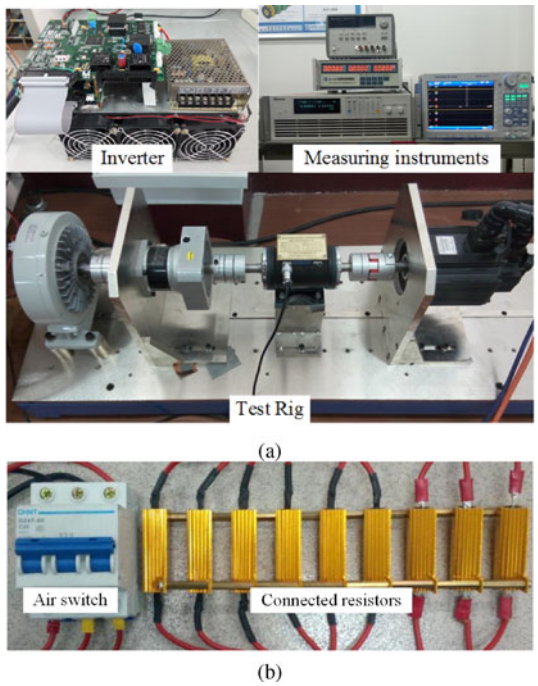

Fig. 10. Experimental devices. (a) Main experimental devices, (b) resistors used to validate online R_s estimation.

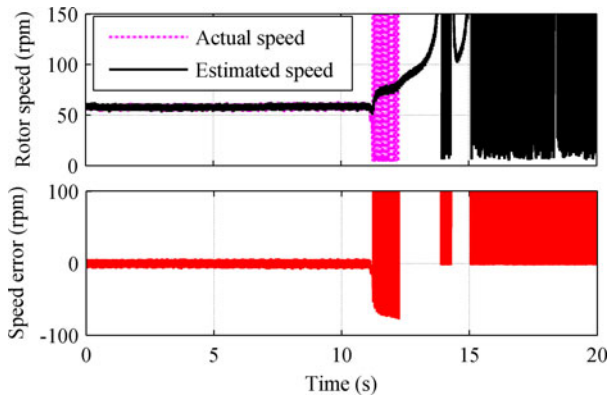

Fig. 11. Rotor speed and speed error without online R_s estimation at speed command of 60 r/min (step change in R_s happens at 12 s).

From what has been discussed above, it can be concluded that stator resistance variation has a great influence on estimation accuracy and robustness of the STA-SMO. The effectiveness of online R_s estimation has been validated by simulations.

VI. Experimental Results and Discussions

The configuration of experimental system is presented in Fig. 10. The PMSM is controlled by a Texas Instruments TMS320F28335 DSP and fed by a Mitsubishi PM75RL1A120 intelligent power module. The switching frequency and sampling frequency of the control system is set to 10 kHz. All of the signals are converted by a digital-to-analog converter DAC7554 and plotted by an oscilloscope.

A. Robustness Verification

In order to validate the effectiveness of the proposed online R_s estimation at low speed operation range, three 0.333 Ω resistors are connected in series with three-phase winding of the PMSM. Step change of R_s is achieved by controlling an air switch, as shown in Fig. 10(b).

Comparison between the STA-SMO without and with R_s estimation is given in Figs. 11 and 12, respectively. Both systems are controlled by the STA-SMO with a 10 N·m load at 60 r/min. It can be seen that after the step change in R_s, the system becomes unstable, as shown in Fig. 11. However, the STA-SMO

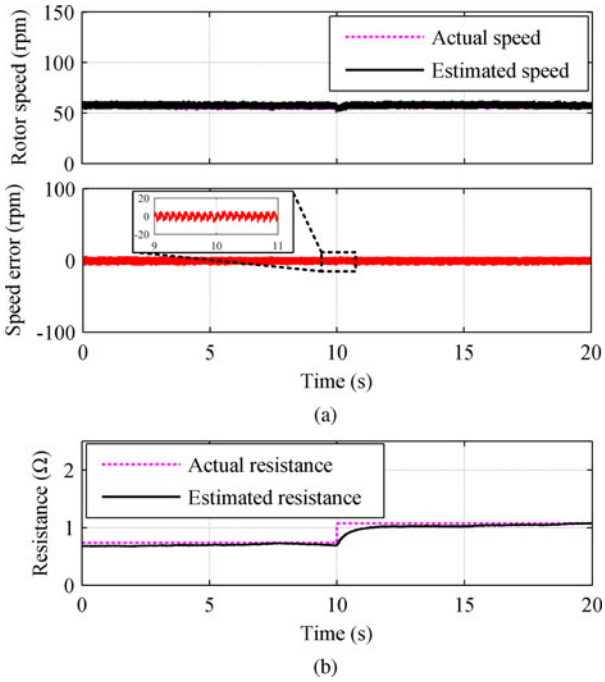

Fig. 12. Rotor speed, speed error, and resistance with proposed online R_s estimation at speed command of 60 r/min (step change in R_s happens at 10 s). (a) Rotor speed and speed error, and (b) actual and estimated R_s.

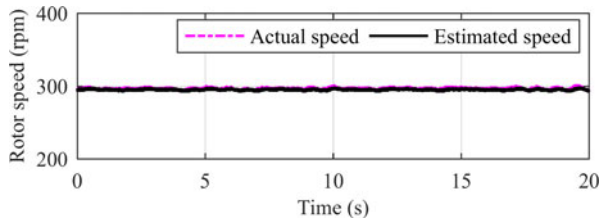

Fig. 13. Rotor speed with online R_s estimation at speed command of 300 r/min (step change in R_s happens at 10 s).

with the proposed online R_s estimation tracks the step change well and the rotor speed error is small after the step change happens. Therefore, system stability can be improved using a more accurate machine model.

The same experiment is conducted at 300 r/min and the experimental result is shown in Fig. 13. It is obvious that stator resistance variation has negligible influence on the sensorless control system. That is because voltage drop across R_s is low compared to back EMF at 300 r/min.

The influence of inductance variation on the STA-SMO sensorless control system is also investigated. The system is controlled by the STA-SMO based sensorless control method with a 10 N·m load at 60 r/min and 300 r/min, respectively. There is a step change of set value from 10.24 to 15.36 mH at 10 s. The experimental results are shown in Fig. 14. It can be seen that inductance variation has little influence on estimation error, as shown in Fig. 14. That is because $L_s \frac{di_{\alpha\beta}}{dt}$ is small at steady state, therefore, the influence of inductance variation can be neglected.

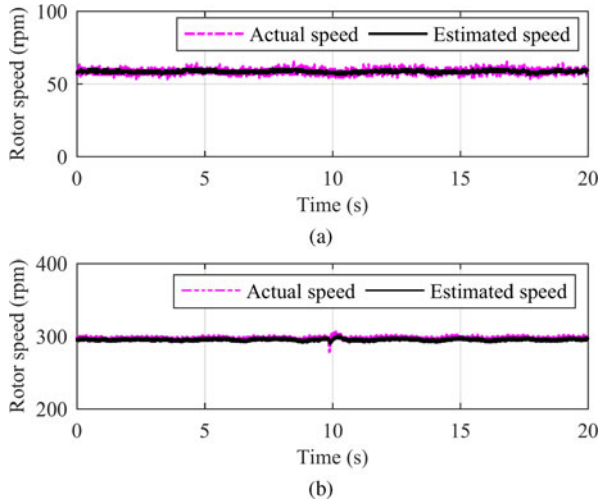

Fig. 14. Rotor speed with online R_s estimation at speed command of 60 r/min and 300 r/min (step change in L_s happens at 10 s). (a) 60 r/min and (b) 300 r/min.

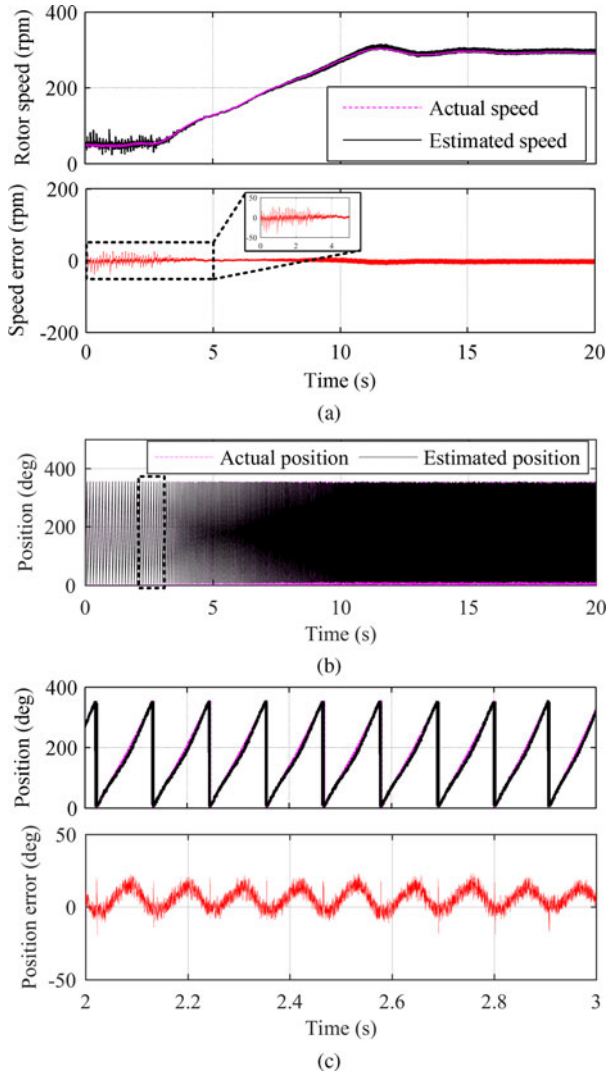

Fig. 15. Acceleration process of first-order SMO-based sensorless control at speed command from 50 to 300 r/min. (a) Rotor speed and speed error, (b) rotor position, and (c) zoomed rotor position and position error.

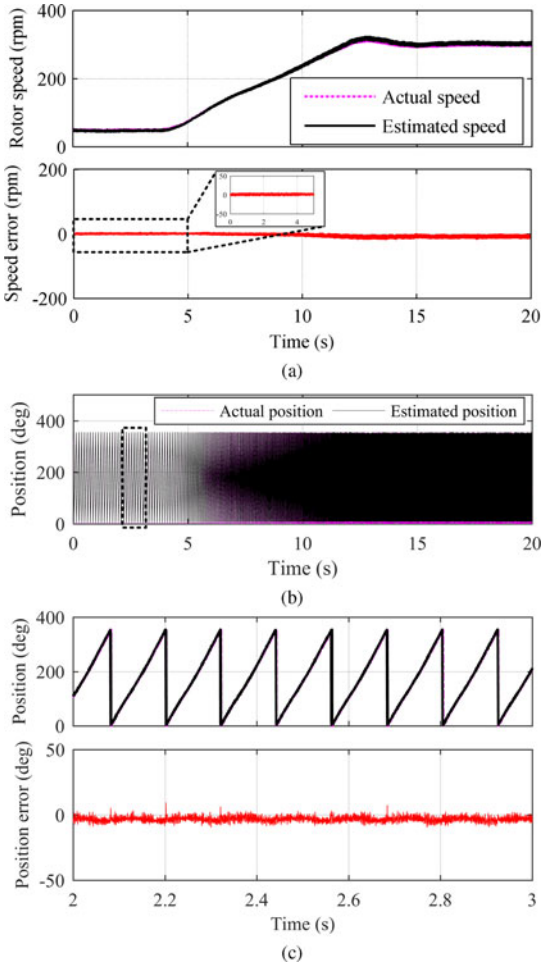

Fig. 16. Acceleration process of an STA-SMO with online R_s estimation based sensorless control at speed command from 50 to 300 r/min. (a) Rotor speed and speed error, (b) rotor position, and (c) zoomed rotor position and position error.

From the above experimental results, it can be concluded that online estimating R_s can improve both estimation accuracy and system stability of the STA-SMO based sensorless control method. Besides, for nonsalient PMSM, influence caused by stator inductance variation can be neglected.

B. Comparison With Conventional First-Order SMO Scheme

In order to validate the effectiveness of proposed scheme, the first-order SMO exhibited in Fig. 1 is used for comparison. The main difference between the first-order SMO and STA-SMO is that the STA-SMO has smaller switching gain, which can reduce chattering greatly. Besides, by estimating R_s online, a more accurate machine model is constructed to obtain higher position estimation accuracy and stronger stability.

The experimental results are shown in Figs. 15 and 16. The PMSM is accelerated from 50 to 300 r/min with a 5 N·m load. The set value of R_s is set to 0.59 Ω (20% smaller than actual R_s). It is obvious that the chattering is eliminated compared to the first-order SMO-based sensorless method. Moreover, the estimated rotor speed and position error of the proposed method is smaller than that of the first-order SMO, especially at low

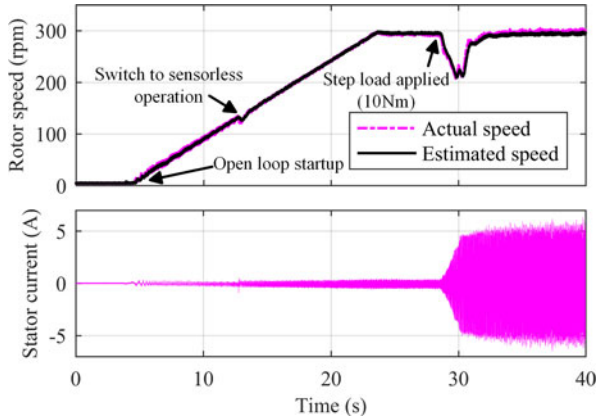

Fig. 17. Dynamic process of the proposed sensorless method.

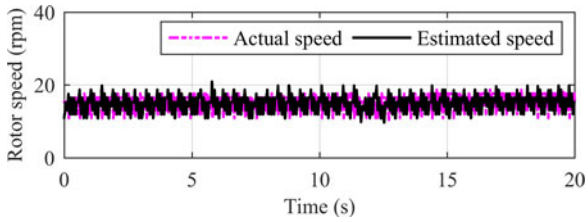

Fig. 18. Low speed operation of the proposed method.

speed region. That is because the voltage drop across R_s cannot be neglected compared to back EMF. However, back EMF is much larger at high speed region, which means the voltage drop across R_s can be ignored. Therefore, speed errors of these two methods at high speed range are almost the same.

From above analysis, it can be concluded that the main contribution of online R_s estimation is the improvement of position estimation accuracy and robustness of the STA-SMO at low speed. Thus, the sensorless operation range can be extended to lower speed.

C. Dynamic Process and Low Speed Operation of the Proposed Method

Since the proposed sensorless scheme is based on a machine model, it cannot operate at zero speed. Therefore, open-loop startup is adopted in this paper. The experimental result is shown in Fig. 17. The PMSM starts up in open loop and switches to sensorless operation at 13 s. Then, a 10 N·m load is enabled at 28 s. It can be seen that the estimated speed tracks the actual speed well at steady state and even dynamic process. Furthermore, the proposed sensorless scheme is intended to operate at 15 r/min. The corresponding experimental result is shown in Fig. 18, while PMSM cannot operate at such a low speed using the conventional first-order SMO-based sensorless control method. The experimental result has verified the high performance of the proposed sensorless control method.

VII. Conclusion

In this paper, sensorless control of surface-mounted PMSM based on the STA-SMO with online R_s estimation is proposed. The chattering problem in a conventional SMO is alleviated by

reducing the amplitude of switching function in an STA-SMO. An online R_s estimation scheme based on a modified SMO is utilized to obtain the accurate machine model. Simulations and experiments are carried out to verify the proposed method. Both simulated and experimental results show that the proposed sensorless technique can eliminate the chattering greatly. Furthermore, with the help of an online R_s observer, estimated rotor position and speed errors are reduced significantly under stator resistance uncertainties, especially at low speed range. In other words, sensorless operation range can be extended to lower speed region by combining the STA-SMO with online R_s estimation. Therefore, it can be concluded that the proposed sensorless control scheme can improve the stability and robustness of the system and achieve wide speed range operation. However, since the proposed method is based on a machine model, it cannot operate at zero speed or ultralow speed. This problem can be solved by combining model-based techniques with anisotropy-based techniques, such as the HF injection method, which is considered to be the future work.

REFERENCES

[1] G. Wang, L. Yang, G. Zhang, X. Zhang, and D. Xu, "Comparative investigation of pseudorandom high-frequency signal injection schemes for sensorless IPMSM drives," *IEEE Trans. Power Electron.*, vol. 32, no. 3, pp. 2123–2132, Mar. 2017.

[2] D. Kim, Y. C. Kwon, S. K. Sul, J. H. Kim, and R. S. Yu, "Suppression of injection voltage disturbance for high-frequency square-wave injection sensorless drive with regulation of induced high-frequency current ripple," *IEEE Trans. Ind. Appl.*, vol. 52, no. 1, pp. 302–312, Jan. 2016.

[3] P. L. Xu and Z. Q. Zhu, "Novel carrier signal injection method using zero-sequence voltage for sensorless control of PMSM drives," *IEEE Trans. Ind. Electron.*, vol. 63, no. 4, pp. 2053–2061, Apr. 2016.

[4] Y. Shi, K. Sun, L. Huang, and Y. Li, "Online identification of permanent magnet flux based on extended Kalman filter for IPMSM drive with position sensorless control," *IEEE Trans. Ind. Electron.*, vol. 59, no. 11, pp. 4169–4178, Nov. 2012.

[5] P. Mercorelli, "A hysteresis hybrid extended Kalman filter as an observer for sensorless valve control in camless internal combustion engines," *IEEE Trans. Ind. Appl.*, vol. 48, no. 6, pp. 1940–1949, Nov. 2012.

[6] P. Mercorelli, "A two-stage augmented extended Kalman filter as an observer for sensorless valve control in camless internal combustion engines," *IEEE Trans. Ind. Electron.*, vol. 59, no. 11, pp. 4236–4247, Nov. 2012.

[7] S. Chi, Z. Zhang, and L. Xu, "Sliding-mode sensorless control of direct-drive pm synchronous motors for washing machine applications," *IEEE Trans. Ind. Appl.*, vol. 45, no. 2, pp. 582–590, Mar. 2009.

[8] H. Kim, J. Son, and J. Lee, "A high-speed sliding-mode observer for the sensorless speed control of a PMSM," *IEEE Trans. Ind. Electron.*, vol. 58, no. 9, pp. 4069–4077, Sep. 2011.

[9] P. Mercorelli, "A two-stage sliding-mode high-gain observer to reduce uncertainties and disturbances effects for sensorless control in automotive applications," *IEEE Trans. Ind. Electron.*, vol. 62, no. 9, pp. 5929–5940, Sep. 2015.

[10] T. Bernardes, V. F. Montagner, H. A. Grndling, and H. Pinheiro, "Discrete-time sliding mode observer for sensorless vector control of permanent magnet synchronous machine," *IEEE Trans. Ind. Electron.*, vol. 61, no. 4, pp. 1679–1691, Apr. 2014.

[11] W. Qiao, X. Yang, and X. Gong, "Wind speed and rotor position sensorless control for direct-drive PMG wind turbines," *IEEE Trans. Ind. Appl.*, vol. 48, no. 1, pp. 3–11, Jan. 2012.

[12] Z. Zhang, Y. Zhao, W. Qiao, and L. Qu, "A space-vector-modulated sensorless direct-torque control for direct-drive PMSG wind turbines," *IEEE Trans. Ind. Appl.*, vol. 50, no. 4, pp. 2331–2341, Jul. 2014.

[13] Z. Qiao, T. Shi, Y. Wang, Y. Yan, C. Xia, and X. He, "New sliding-mode observer for position sensorless control of permanent-magnet synchronous motor," *IEEE Trans. Ind. Electron.*, vol. 60, no. 2, pp. 710–719, Feb. 2013.

[14] Y. Zhao, W. Qiao, and L. Wu, "An adaptive quasi-sliding-mode rotor position observer-based sensorless control for interior permanent magnet synchronous machines," *IEEE Trans. Power Electron.*, vol. 28, no. 12, pp. 5618–5629, Dec. 2013.

[15] D. Liang, J. Li, and R. Qu, "Super-twisting algorithm based sliding-mode observer with online parameter estimation for sensorless control of permanent magnet synchronous machine," in *Proc. 8th IEEE Energy Convers. Congr. Expo.*, Sep. 2016, pp. 1–8.

[16] M. Pacas, "Sensorless drives in industrial applications," *IEEE Ind. Electron. Mag.*, vol. 5, no. 2, pp. 16–23, Jun. 2011.

[17] G. Foo and M. F. Rahman, "Sensorless sliding-mode MTPA control of an IPM synchronous motor drive using a sliding-mode observer and HF signal injection," *IEEE Trans. Ind. Electron.*, vol. 57, no. 4, pp. 1270–1278, Apr. 2010.

[18] J. P. V. Cunha, R. R. Costa, F. Lizarralde, and L. Hsu, "Peaking free variable structure control of uncertain linear systems based on a high-gain observer," *Automatica*, vol. 45, no. 5, pp. 1156–1164, 2009.

[19] L. Zhao, J. Huang, H. Liu, B. Li, and W. Kong, "Second-order sliding-mode observer with online parameter identification for sensorless induction motor drives," *IEEE Trans. Ind. Electron.*, vol. 61, no. 10, pp. 5280–5289, Oct. 2014.

[20] A. Levant, "Sliding order and sliding accuracy in sliding mode control," *Int. J. Control*, vol. 58, no. 6, pp. 1247–1263, 1993.

[21] A. Levant, "Principles of 2-sliding mode design," *Automatica*, vol. 43, no. 4, pp. 576–586, 2007.

[22] J. A. Moreno and M. Osorio, "A Lyapunov approach to second-order sliding mode controllers and observers," in *Proc. 47th IEEE Conf. Decis. Control*, Dec. 2008, pp. 2856–2861.

[23] M. Ezzat, J. de Leon, N. Gonzalez, and A. Glumineau, "Observer-controller scheme using high order sliding mode techniques for sensorless speed control of permanent magnet synchronous motor," in *Proc. 49th IEEE Conf. Decis. Control*, Dec. 2010, pp. 4012–4017.

[24] S. D. Gennaro, J. Rivera, and B. Castillo-Toledo, "Super-twisting sensorless control of permanent magnet synchronous motors," in *Proc. 49th IEEE Conf. Decis. Control*, Dec. 2010, pp. 4018–4023.

[25] Y. Inoue, Y. Kawaguchi, S. Morimoto, and M. Sanada, "Performance improvement of sensorless IPMSM drives in a low-speed region using online parameter identification," *IEEE Trans. Ind. Appl.*, vol. 47, no. 2, pp. 798–804, Mar. 2011.

[26] K. Liu, Z. Q. Zhu, and D. A. Stone, "Parameter estimation for condition monitoring of PMSM stator winding and rotor permanent magnets," *IEEE Trans. Ind. Electron.*, vol. 60, no. 12, pp. 5902–5913, Dec. 2013.

[27] K. Liu and Z. Q. Zhu, "Position-offset-based parameter estimation using the adaline NN for condition monitoring of permanent-magnet synchronous machines," *IEEE Trans. Ind. Electron.*, vol. 62, no. 4, pp. 2372–2383, Apr. 2015.

[28] Z. Yan and V. Utkin, "Sliding mode observers for electric machines—An overview," in *Proc. 28th IEEE Ann. Conf. Ind. Electron. Soc.*, vol. 3, Nov. 2002, pp. 1842–1847.

[29] V. I. Utkin, J. Guldner, and J. Shi, *Sliding Mode Control in Electro-Mechanical Systems*. Boca Raton, FL, USA: CRC Press, 2009.

[30] A. Levant, "Robust exact differentiation via sliding mode technique," *Automatica*, vol. 34, no. 3, pp. 379–384, 1998.

[31] J. A. Moreno and M. Osorio, "Strict Lyapunov functions for the super-twisting algorithm," *IEEE Trans. Autom. Control*, vol. 57, no. 4, pp. 1035–1040, Apr. 2012.

[32] J. Davila, L. Fridman, and A. Levant, "Second-order sliding-mode observer for mechanical systems," *IEEE Trans. Autom. Control*, vol. 50, no. 11, pp. 1785–1789, Nov. 2005.

[33] V. I. Utkin, *Sliding Modes in Control and Optimization*. New York, NY, USA: Springer, 1992.

Donglai Liang (S'15) was born in Guangdong, China in 1990. He received the B.E.E. degree from the Huazhong University of Science and Technology, Wuhan, China, in 2013. He is currently working toward the Ph.D. degree in electrical engineering from the School of Electronic and Electrical Engineering, Huazhong University of Science and Technology.

His research interest focuses on PM machine design and control.

Jian Li (M'10) received the B.E.E degree from the Dalian University of Technology, Dalian, China, in 2005, and the M.S.E.E and Ph.D. degrees in electrical engineering from Dong-A University, Busan, South Korea, in 2007 and 2011, respectively.

He is currently an Associate Research Professor in the School of Electrical and Electronic Engineering, Huazhong University of Science and Technology, Wuhan, China. His research interests include design and control of PM machines, and reluctance machines.

Ronghai Qu (S'01–M'02–SM'05) was born in China. He received the B.E.E. and M.S.E.E. degrees from Tsinghua University, Beijing, China, in 1993 and 1996, respectively, and the Ph.D. degree in electrical engineering from the University of Wisconsin-Madison, Madison, WI, USA, in 2002.

In 1998, he joined the Wisconsin Electric Machines and Power Electronics Consortiums as a Research Assistant. He became a Senior Electrical Engineer with Northland, a Scott Fetzer Company, in 2002. In 2003, he joined the General Electric (GE) Global Research Center, Niskayuna, NY, USA, as a Senior Electrical Engineer with the Electrical Machines and Drives Laboratory. Since 2010, he has been a Professor with the Huazhong University of Science Technology, Wuhan, China. He has authored more than 120 published technical papers and is the holder of more than 50 patents/patent applications.

Prof. Qu is a full member of Sigma Xi. He has received several awards from the GE Global Research Center since 2003, including technical achievement and management awards. He also received the third prize in 2003 and 2005 Best Paper Awards, from the Electric Machines Committee of the IEEE Industry Applications Society at the 2002 and 2004 IAS Annual Meeting, respectively.